

Chapter 4

3D Printed Microfluidic Devices

Gregory W. Bishop

1 Introduction

Recently, increasing interest has developed around the use of 3D printing methods for the preparation of microfluidic devices. 3D printing generally involves deposition or curing of materials in a layer-by-layer fashion as determined by a three-dimensional representation of the desired object. While 3D printing was invented and first demonstrated in the 1980s, prohibitive costs and the limited number of commercially available printers and materials restricted applications to rapid prototyping for manufacturing. Present-day enthusiasm surrounding 3D printing can largely be attributed to momentum established about a decade ago by initiatives such as the RepRap and Fab@Home Projects [1, 2]. These endeavors have provided great progress toward democratizing 3D printing by promoting interest in technology, fostering collaboration through communities of enthusiasts, and decreasing barriers associated with high costs and levels of expertise. Improvements in affordability and accessibility of 3D printers have enabled new applications in many fields, including medicine and biotechnology. 3D printing is especially attractive for the fabrication of microfluidic devices due to its rapid prototyping capabilities and simple procedure compared to other previously described methods, which are more time-consuming and typically require a greater amount of expertise and expensive equipment [1, 3].

G.W. Bishop (✉)

Department of Chemistry, East Tennessee State University, Johnson City, TN, USA

e-mail: bishopgw@etsu.edu

2 3D Printing Techniques

3D printing offers fast design-to-object workflow and typically requires few, relatively simple steps. First, a computer-aided design (CAD) file is generated through the use of CAD software or by computer-assisted scanning of a real object. Free CAD programs and online libraries that allow users to share CAD files have provided means for increased utilization of 3D printing technologies. Printer instructions are generated by a slicer program, which separates the CAD file into sections along the vertical axis to define the composition of each printed layer. After uploading the instructions to the printer, the object is fabricated on a platform via a controlled deposition or curing apparatus interfaced with a precise positioning system. Finally, the printed object is removed from the platform. Depending on the printing method and parameters defined in the slicer program, post-processing may be necessary to remove extraneous material and supports used to bolster the structural integrity of the printed layers during the fabrication process.

Generally, layer fabrication in 3D printing is accomplished by deposition of thermoplastics (fused deposition modeling) or viscoelastic materials (syringe deposition or direct ink writing) through a nozzle or syringe, sintering of powdered materials (selective laser sintering), exposure of photocurable resin contained in a reservoir (stereolithography), or inkjet printing of photocurable inks followed by immediate exposure (PolyJet or MultiJet) [4–6]. Some important aspects for printing methods relevant to fluidic device fabrication are briefly described in this section.

2.1 *Extrusion-Based Methods*

In fused deposition modeling (FDM), a thermoplastic filament (typically 1.75 or 3.00 mm in diameter) is extruded through a heated nozzle (typically ~0.2–0.5 mm in diameter) onto a moving platform (Fig. 4.1). The extruder assembly (Fig. 4.1b) is often mounted on a gantry system that controls XY movement, and the platform or stage moves in the Z direction. Fabrication of single objects composed of multiple materials can easily be accomplished with this method simply by including more than one extruder nozzle in the printer design. Typical filament materials include poly(lactic acid), acrylonitrile butadiene styrene, and poly(carbonate). However, there is a great deal of interest in developing composite materials with improved physical and chemical characteristics for various applications. Composite filaments that incorporate carbon nanotubes, graphene, ceramics, and magnetic materials are commercially available.

Direct ink writing, pioneered by Lewis et al., is another extrusion-based technique for 3D printing [7]. Direct ink writing uses a pneumatically controlled syringe to print viscoelastic materials, such as colloidal suspensions of nanoparticles, polymers, and ceramics, onto a moving platform [7–13]. Rheological properties

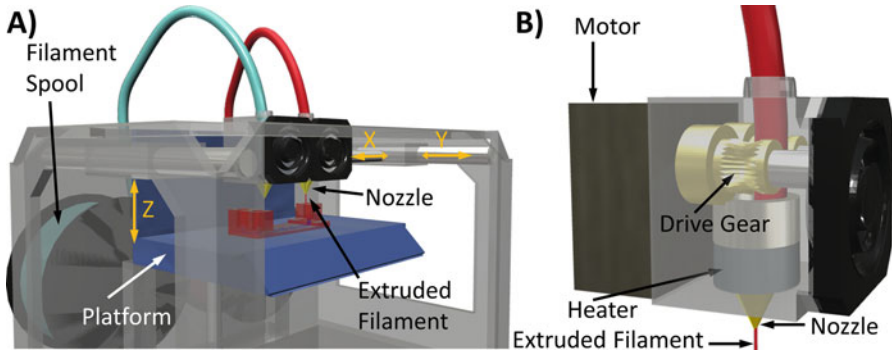


Fig. 4.1 Illustrated representation of an FDM-based 3D printer. (a) Object is printed from extruded filament deposited on a moving platform. Extruder assembly is mounted on a gantry system that controls deposition in the X and Y directions. (b) Close-up view of the extruder assembly. Adapted from Reference [6] with permission from IOP Publishing

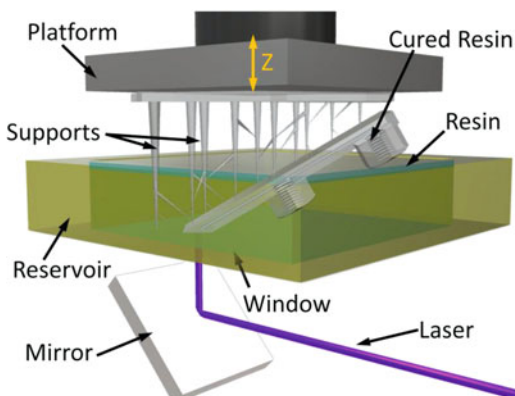
of viscoelastic inks are tailored to facilitate extrusion through syringes with diameters as small as $1\ \mu\text{m}$ [9].

2.2 Methods Based on Photocuring

In stereolithography (SLA), photocurable resin held in a reservoir is exposed to a light source. In the traditional form of SLA, a laser is scanned in a pattern defined by the slicer program to cure each layer onto a moving platform (Fig. 4.2). Some SLA printers now incorporate projection systems such as a digital mirror device to facilitate curing of layers with single exposure steps. Digital light processing (DLP) projectors that feature ultra-high performance lamps or light emitting diodes permit fabrication of objects with greater detail since XY resolution is limited by pixel size [14] ($\sim 30\ \mu\text{m}$ for 920×1140 pixels) rather than laser spot size (often $\sim 100\ \mu\text{m}$) [15]. However, printing with improved resolution limits the overall object size since DLPs possess a fixed number of pixels. SLA materials are limited to acrylate- and epoxy-based resins [4], and fabrication of single objects composed of more than one material is not easily accomplished.

Recently, Tumbleston et al. described a 3D printer based on a process called continuous liquid interface production (CLIP) [16]. CLIP is similar to SLA in its operation; however, CLIP uses an oxygen permeable membrane between the optical window and cured part. The presence of the membrane leads to a controllable oxygen-containing layer where photopolymerization of the resin is not permitted. This enables the exposure, replacement of resin, and movement of cured part processes to be performed in a continuous manner instead of as discrete steps as they are in traditional SLA. CLIP has been shown to reduce printing times from hours to minutes over traditional SLA.

Fig. 4.2 Illustrated representation of a laser SLA-based 3D printer. Adapted from Reference [6] with permission of IOP Publishing



Like SLA, MultiJet and PolyJet technologies also employ photocurable materials. However, these methods rely on inkjet printing and immediate exposure to harden each layer. MultiJet and PolyJet printers are outfitted with multiple print-heads so objects composed of more than one material can be produced.

2.3 Cost and Materials

Printers based on each of these techniques are commercially available. Depending on the printing method and capabilities, 3D printers range in price from <\$1000–\$100,000 USD or more. Printers based on FDM are typically among the lowest in cost with some SLA printers also approaching a consumer-grade price-point. Printers based on PolyJet and MultiJet technologies are among the most expensive. There are also several commercial services that enable customers to submit CAD files to receive corresponding printed objects prepared by a high-resolution 3D printer [3, 17–19]. Likewise, commercially available materials also vary in cost with prices for thermoplastic filaments ranging from ~\$30/kg or more and photo-polymer materials for SLA and inkjet-based technologies starting at ~\$120/L. Many of the commercially available materials for SLA-based 3D printing are not biocompatible [5]. However, there are a growing number of biocompatible options as interest in materials development continues to be a focus for extending the capabilities of various 3D printing technologies.

3 3D-Printed Microfluidics

Various methods and applications of milli- and microfluidic devices have been described. Due to the inadequate resolution of many 3D printers, the limiting dimensions of the 3D-printed fluidic channels are typically on the order of tens to

a few hundred micrometers. Therefore, many 3D-printed “microfluidic” devices described in recent literature are given this distinction to convey the microliter to sub-microliter volumes they contain. Very few reports of 3D-printed “microfluidic” devices correspond to channels with micrometer dimensions characteristic of true microfluidics. While 3D printing can be used to make small features, it is not yet routine for most current technologies to fabricate objects that include design elements of different vastly scale, such as microfluidic devices with submicrometer channels in housings of several centimeters. However, progress continues to push the boundaries of 3D printing towards capabilities necessary for true microfluidic devices.

3.1 Molds and Scaffolds for Fluidic Channels

The first applications of 3D printing to fluidics involved the production of molds for elastomer-based microfluidics. Unlike photolithography, which requires the production of a mask to create the master mold, 3D printing enables fabrication of the master directly from the design file. These techniques also facilitate the preparation of complex molds for channels that propagate in all three dimensions. Such molds would be difficult or impossible to produce by two-dimensional photolithography, since they require multiple masks and layer bonding.

Whitesides et al. demonstrated that a printer based on FDM could be used to prepare molds for PDMS channels with limiting dimensions of 250 μm or more [20]. Channel dimensions are limited by nozzle size, and the surface roughness of FDM-printed objects is quite large ($\sim 8 \mu\text{m}$) since each printed layer is essentially composed of adjacent cylindrical threads of thermoplastic filament. Molds produced by SLA exhibit surface roughness of $< 1 \mu\text{m}$ and can be used to produce PDMS channels with dimensions of $\sim 50 \mu\text{m}$ [21, 22]. Mixing channels and channels with integrated valves prepared from 3D-printed molds have been demonstrated [20–22].

Microvasculature scaffolds for epoxy-based fluidic devices have been prepared by direct ink writing [8]. A pneumatically controlled syringe with diameter as small as 10 μm is employed to produce the scaffold from fugitive organic inks (Prussian blue paste). After curing, the scaffold is removed by heating to 60 $^{\circ}\text{C}$ under light vacuum. Fluidic devices with remarkably smooth cylindrical channels (surface roughness $13.3 \pm 6.5 \text{ nm}$) result. Similarly, FDM has been used to prepare scaffolds from acrylonitrile butadiene styrene (ABS) for PDMS-based fluidic devices [23]. ABS dissolves in acetone, permitting its removal from cured PDMS.

3.2 *Fluidic Devices Prepared by Direct Printing*

Direct fabrication of 3D-printed fluidic devices has also been demonstrated. Channels with limiting dimensions of $\sim 500\text{--}800\ \mu\text{m}$ have been produced from poly(propylene), poly(lactic acid), and poly(ethylene terephthalate) by FDM [24]. As previously stated, FDM-printed objects are composed of layers of adjacent cylindrical threads, which results in channels with ridged or scalloped internal surfaces [5]. Additionally, the overlap of adjacent layers makes it difficult to visualize fluids contained within the channel even when clear filaments are used [25]. Fluids in channels are largely obscured when located beneath 14 or more printed layers (0.200 mm) of clear PET filament. Better visualization of fluids within channels can be obtained by printing the bottom layer of the device on a heated platform, which reduces surface roughness.

Printers based on photocurable inks and resins can produce channels with typical limiting dimensions of $\sim 250\ \mu\text{m}$ [26, 27]. Smaller channels are also possible; however, it is often difficult to remove necessary support material from smaller channels. For example, during SLA, the channel is filled with uncured resin, which can be difficult to force from small channels. Also, since some light can reach uncured resin held within the channel during the printing process, complete blockage of the channel can result in some areas. The surface roughness of 500 μm -high channels printed by SLA was reported to be $\sim 2.54\ \mu\text{m}$ [3], and a study of four different 3D printers based on inkjet technologies found surface roughness to range from $\sim 0.09\text{--}2.24\ \mu\text{m}$ [28].

Nordin et al. investigated the effect of resin composition on limiting channel dimensions produced by DLP-SLA [14]. Resins for SLA usually consist of monomer material(s), a photoinitiator, and an absorber, which is included to control the penetration depth of the light source. Nordin et al. found that controlling the penetration depth by using higher concentrations of the absorber was crucial for production of small channels. 60 μm -high channels were printed with 100% yield using a custom-formulated resin that contained poly(ethylene glycol) diacrylate (PEGDA), 1% photoinitiator phenylbis(2,4,6-trimethylbenzoyl)phosphine oxide (Irgacure 819), and 0.6% absorber Sudan I. For 100% success rate, width for these channels must be at least 108 μm (4 pixels) as determined by the limitations of the 912×1140 pixel DLP projector.

Due to the availability of clear resins and inks, 3D printed fluidic devices prepared by SLA and inkjet technologies can also permit visualization of fluids within the channels. As-printed, devices are typically opaque and must be processed to improve transparency. For example, the outer layers of SLA-printed devices can be sanded with up to 2000-grit sand paper, polished with a plastic cleaning compound, and coated with clear acrylic spray to enhance clarity [29, 30].

Photopolymer-based 3D-printing methods possess sufficient resolution to produce complex fluidics and modular fluidic devices. SLA has been used to prepare channels with integrated membrane-based valves that can be pneumatically controlled [27, 31]. SLA and MultiJet printing have been employed to yield

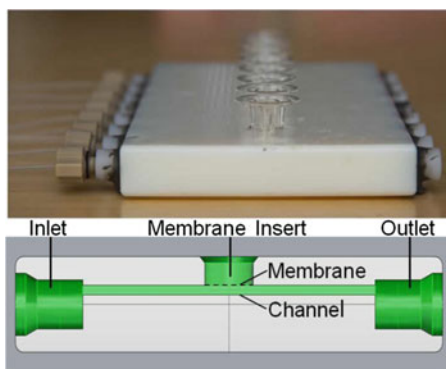
microfluidic components that can be reversibly connected to construct customizable fluidics [18, 19]. Channels can also be filled with fast-drying, conductive suspensions of colloidal silver to make resistors and inductors for electrical circuits and wireless sensors [32].

4 3D-Printed Fluidics and Bioanalysis

3D-printed fluidic devices have been described for use in cell studies and measurements of biomolecules and biologically relevant species. With relatively high resolution printers based on SLA and inkjet methods, threaded ports can be printed to interface the channel with commercially available fittings and tubing for easy access [33]. Spence et al. have employed a PolyJet printer to produce various fluidic devices that feature access ports for reversibly integrating commercially available membrane inserts and other components into channels for various cell studies [29, 33–35] (Fig. 4.3). Membrane inserts selectively transport small molecules from the channel and prohibit transport of larger species like large biomolecules and cells. In one cell viability study, a layer of bovine pulmonary artery endothelial cells was deposited on a cell culture membrane inserted into the 3D-printed channel [33]. Saponin (a detergent that disrupts the cell membrane) or Hank's balanced salt solution (HBSS) was delivered into the fluidic channel. Sytox Green staining of cells indicated that a larger population of dead cells resulted upon exposure of cells in the membrane to saponin compared to HBSS.

Fluidic devices have also been designed such that a commercial plate reader can be used to perform measurements [34]. Such platforms have enabled investigation of the effects of storage conditions related to transfusion medicine on ATP production by erythrocytes. Erythrocytes stored in FDA-approved additive solution 1 (AS-1) that contains ~110 mM glucose or a modified AS-1 with lower glucose concentration (5.5 mM) were delivered into the 3D-printed channel. Membrane inserts provided reservoirs for collecting and measuring adenosine triphosphate

Fig. 4.3 3D-printed fluidic device used in cell studies. Device features 3 mm wide \times 1.5 mm deep channels for incorporating membrane inserts. Reprinted with permission from Reference [33], Copyright 2013 American Chemical Society



(ATP) transported from the channel. Erythrocytes stored in the modified AS-1 exhibited greater ATP production than those stored in commonly used AS-1.

In addition to membrane inserts, sensing elements like electrodes and optical fibers have also been incorporated into 3D-printed channels to facilitate bioanalytical measurements [17, 25, 28, 30, 35–37] (Fig. 4.4). Electrodes can be fastened in channels through access holes, deposited on substrates that are bound to open-sided channels to complete the fluidic device, or housed in threaded fittings that are compatible with threaded ports included in the device design. 0.5 mm carbon and platinum electrodes incorporated in 3D-printed channels have been used to detect viruses that were labeled with cadmium sulfide quantum dots [36]. Dopamine, nitric oxide, ATP, and hydrogen peroxide have also been measured using 3D-printed fluidic devices with integrated electrodes [25, 35]. Continuous monitoring of glucose and lactate in human subjects during and after physical activity was accomplished by connecting an FDA-approved microdialysis probe to a 3D-printed channel ($375\ \mu\text{m} \times 508\ \mu\text{m}$, internal volume $1.9\ \mu\text{L}$) equipped with needle electrode biosensors [37].

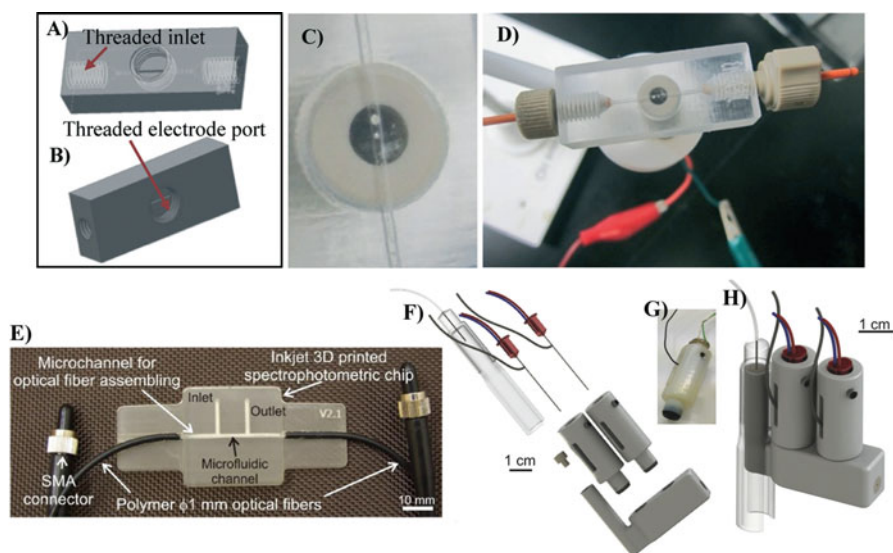


Fig. 4.4 3D-printed channels with integrated devices. (a–d) Schematic (a, b) and photographs (c, d) of a device that features a threaded port for incorporating disk-shaped electrodes into a $500\ \mu\text{m}$ diameter channel. Reproduced from Reference [35] with permission from the Royal Society of Chemistry. (e) Photograph of fluidic channel interfaced with optical fibers for in-channel spectrophotometry. Reproduced from reference [28] with permission from IOP Publishing. (f–h) Fluidic device with integrated needle biosensors for continuous monitoring of glucose and lactate from dialysate. Reproduced by the permission from Reference [37]; copyright American Chemical Society

5 Outlook and Prospects

Growing interest in 3D printing techniques and improvements in technological capabilities and materials have resulted in many new applications. Due to the simple and fast design-to-object workflow, 3D printing offers advantages over traditional fabrication techniques for the production of microfluidic devices. Fluidic devices can be directly printed from CAD files that are processed using slicer software, and several free and open-source design and slicer programs are available. The printing process allows more freedom in design than other fabrication techniques to a certain extent due to the ability to produce channels that propagate in various directions. Also, several device designs can be produced and tested relatively quickly, since there is no need to prepare various masks and molds that are required with other techniques. Currently, there are few 3D printing techniques that can produce channels with dimensions $<100\ \mu\text{m}$; however, as the capabilities of 3D printing continue to improve, so too will these boundaries. Applications of 3D-printed fluidic devices have shown their utility and robustness in bioanalytical applications, including cell studies, biomolecule sensing, and immunoassays.

References

1. Waldbaur A, Rapp H, Länge K, Rapp BE (2011) Let there be chip—towards rapid prototyping of microfluidic devices: one step manufacturing processes. *Anal Meth* 3:2681–2716
2. Ventola CL (2014) Medical applications for 3D printing: current and projected uses. *Pharmacol Ther* 39:704–711
3. Au AK, Lee W, Folch A (2014) Mail-order microfluidics: evaluation of stereolithography for the production of microfluidic devices. *Lab Chip* 14:1294–1301
4. Gross BC, Erkal JL, Lockwood SY, Chen C, Spence DM (2014) Evaluation of 3D printing and its potential impact on biotechnology and the chemical sciences. *Anal Chem* 86:3240–3253
5. O'Neill PF, Azouz AB, Vázquez M, Liu J, Marczak S, Slouka Z, Chang HC, Diamond D, Brabazon D (2014) Advances in three-dimensional rapid prototyping of microfluidic devices for biological applications. *Biomicrofluidics* 8:052112
6. Bishop GW, Satterwhite-Warden JE, Kadimisetty K, Rusling JF (2016) 3D printed bioanalytical devices. *Nanotechnology* 27:284002
7. Lewis JA (2006) Direct ink writing of 3D functional materials. *Adv Funct Mater* 16:2193–2204
8. Theriault D, White S, Lewis JA (2003) Chaotic mixing in three-dimensional microvascular networks fabricated by direct-write assembly. *Nat Mater* 2:265–271
9. Ahn BY, Duoss EB, Motala MJ, Guo X, Park S-I, Xiong Y, Yoon J, Nuzzo RG, Rogers JA, Lewis JA (2009) Omnidirectional printing of flexible, stretchable, and spanning silver microelectrodes. *Science* 323:1590–1593
10. Wu W, DeConinck A, Lewis JA (2011) Omnidirectional printing of 3D microvascular networks. *Adv Mater* 23:H178–H183
11. Sun K, Wei T-S, Ahn BY, Seo JY, Dillon SJ, Lewis JA (2013) 3D printing of interdigitated Li-ion microbattery architectures. *Adv Mater* 25:4539–4543
12. Compton BG, Lewis JA (2014) 3D-printing of lightweight cellular composites. *Adv Mater* 26:5930–5935

13. Muth JT, Vogt DM, Truby RL, Mengüç Y, Kolesky DB, Wood RJ, Lewis JA (2014) Embedded 3D printing of strain sensors within highly stretchable elastomers. *Adv Mater* 26:6307–6312
14. Gong H, Beauchamp M, Perry S, Woolley AT, Nordin GP (2015) Optical approach for resin formulation for 3D printed microfluidics. *RSC Adv* 5:106621–106632
15. Ho CMB, Ng SH, Li KHH (2015) 3D printed microfluidics for biological applications. *Lab Chip* 15:3627–3637
16. Tumbleston JR, Shirvanyants D, Ermoshkin N, Januszewicz R, Johnson AR, Kelly D, Chen K, Pinschmidt R, Rolland JP, Ermoshkin A, Samulski ET, DeSimone JM (2015) Science 347:1349–1352
17. Snowden ME, King PH, Covington JA, Macpherson J, Unwin PR (2010) Fabrication of versatile channel flow cells for quantitative electroanalysis using prototyping. *Anal Chem* 82:3124–3131
18. Lee KG, Park KJ, Seok S, Shin S, Kim DH, Park JY, Heo YS, Lee SJ, Lee TJ (2014) 3D printed modules for integrated microfluidic devices. *RSC Adv* 4:32876–32880
19. Bhargava KC, Thompson B, Malmstadt N (2014) Discrete elements for 3D microfluidics. *Proc Natl Acad Sci* 111:15013–15018
20. McDonald JC, Chabinyc ML, Metallo SJ, Anderson JR, Stroock AD, Whitesides GM (2002) Prototyping of microfluidic devices in poly(dimethylsiloxane) using solid-object printing. *Anal Chem* 74:1537–1545
21. Comina G, Suska A, Filippini D (2014) PDMS lab-on-a chip fabrication using 3D printed templates. *Lab Chip* 14:424–430
22. Chan HN, Chen Y, Shu Y, Chen Y, Tian Q, Wu H (2015) Direct, one-step molding of 3D-printed structures for convenient fabrication of truly 3D PDMS microfluidic chips. *Microfluid Nanofluid* 19:9–18
23. Saggiomo V, Velders AH (2015) Simple 3D printed scaffold-removal method for the fabrication of intricate microfluidic devices. *Adv Sci* 2:1500125
24. Kitson PJ, Rosnes MH, Sans V, Dragone V, Cronin L (2012) Configurable 3D-printed millifluidic and microfluidic ‘lab on a chip’ reaction ware devices. *Lab Chip* 12:3267–3271
25. Bishop GW, Satterwhite JE, Bhakta S, Kadimisetty K, Gillette KM, Rusling JF (2015) 3D-printed fluidic devices for nanoparticle preparation and flow-injection amperometry using integrated Prussian blue nanoparticle-modified electrodes. *Anal Chem* 87:5437–5443
26. Shallan AI, Smejkal P, Corban M, Guijt RM, Breadmore MC (2014) Cost-effective three-dimensional printing of visibly transparent microchips within minutes. *Anal Chem* 86:3124–3130
27. Rogers CI, Qaderi K, Woolley AT, Nordin GP (2015) 3D printed microfluidic devices with integrated valves. *Biomicrofluidics* 9:016501
28. Walczak R, Adamski K (2015) Inkjet 3D printing of microfluidic structures—on the selection of the printer towards printing your own microfluidic chips. *J Micromech Microeng* 25:085013
29. Gross BC, Anderson KB, Meisel JE, McNitt MI, Spence DM (2015) Polymer coatings in 3D-printed fluidic device channels for improved cellular adherence prior to electrical lysis. *Anal Chem* 87:6335–6341
30. Bishop GW, Satterwhite-Warden JE, Bist I, Chen E, Rusling JF (2016) Electrochemiluminescence at bare and DNA-coated graphite electrodes in 3D-printed fluidic devices. *ACS Sens* 1(2):197–202
31. Au AK, Bhattacharjee N, Horowitz LF, Chang TC, Folch A (2015) 3D-printed microfluidic automation. *Lab Chip* 15:1934–1941
32. Wu S-Y, Yang C, Hsu W, Lin L (2015) 3D-printed microelectronics for integrated circuitry and passive wireless sensors. *Microsys Nanoeng* 1:15013
33. Anderson KB, Lockwood SY, Martin RS, Spence DM (2013) A 3D printed fluidic device that enables integrated features. *Anal Chem* 85:5622–5626

34. Chen C, Wang Y, Lockwood SY, Spence DM (2014) 3D-printed fluidic devices enable quantitative evaluation of blood components in modified storage solutions for use in transfusion medicine. *Analyst* 139:3219–3226
35. Erkal JL, Selimovic A, Gross BC, Lockwood SY, Walton EL, McNamara S, Martin RS, Spence DM (2014) 3D printed microfluidic devices with integrated versatile and reusable electrodes. *Lab Chip* 14:2023–2032
36. Krejcova L, Nejdil L, Rodrigo MAM, Zurek M, Matousek M, Hynek D, Zitka O, Kopel P, Adam V, Kizek R (2014) 3D printed chip for electrochemical detection of influenza virus labelled with CdS quantum dots. *Biosens Bioelectron* 54:421–427
37. Gowers SAN, Curto VF, Seneci CA, Vadgama P, Yang G-Z, Boutelle MG (2015) 3D printed microfluidic device with integrated biosensors for analysis of subcutaneous human microdialysate. *Anal Chem* 87:7763–7770